QUANTUM CELLULAR AUTOMATA

Craig S. Lent, P. Douglas Tougaw, Wolfgang Porod, and Gary H. Bernstein

Department of Electrical Engineering
University of Notre Dame
Notre Dame, IN 46556

Abstract

We formulate a new paradigm for computing with cellular automata (CA) composed of arrays of quantum devices — quantum cellular automata. Computing in such a paradigm is *edge-driven*. Input, output, and power are delivered at the edge of the CA array only; no direct flow of information or energy to internal cells is required. Computing in this paradigm is also *computing with the ground-state*. The architecture is so designed that the ground state configuration of the array, subject to boundary conditions determined by the input, yields the computational result. We propose a *specific realization* of these ideas using two-electron cells composed of quantum dots, which is within the reach of current fabrication technology. The charge density in the cell is very highly polarized (aligned) along one of the two cell axes, suggestive of a two-state CA. The polarization of one cell induces a polarization in a neighboring cell through the Coulomb interaction in a very nonlinear fashion. Quantum cellular automata can perform useful computing. We show that AND gates, OR gates, and inverters can be constructed and interconnected.

1. Introduction

The continual down-scaling of device dimensions in microelectronics technology has led to faster devices and denser circuit arrays with obvious benefits to chip performance. Dramatic as they have been, these changes have been evolutionary in nature in that even the most advanced chips use the same paradigms for computing as their more primitive ancestors. There is now much expectation that the availability of very dense device arrays might lead to new paradigms for information processing based on locally-interconnected architectures such as cellular automata (CA) and cellular neural networks [1].

There has also been considerable interest in quantum mesoscopic structures for their possible application as devices[2]. Much has been learned about the behavior of electrons flowing through very small structures in semiconductors. Various investigators have pointed out the natural link between mesoscopic quantum systems and cellular automata architectures [3,4,5]. Because quantum structures are necessarily so small, it is difficult to conceive of a regime in which a single quantum device could drive many other devices in subsequent stages [6]. Furthermore, the capacitance of ultra-small wires forming the connections to each device would tend to dominate the behavior of an assembly of quantum devices. For these reasons locally interconnected structures such as cellular neural networks and cellular automata may provide the natural architecture for quantum devices.

We focus here on the idea of employing cellular automata (CA) architectures which are compatible with nanometer-scale quantum devices — thus, *quantum cellular automata* (QCA). A quantum cellular automaton would consist of an array of quantum device cells in a locally-interconnected architecture. The cell state becomes identified with the quantum state of the mesoscopic device. Two-state CA's are attractive because they naturally admit to encoding binary information. For a two-state QCA, each cell should have two stable quantum states. The state of a given cell should influence the state of the

neighboring cells. Two ingredients are essential then: 1) the bistability of the cell, and 2) coupling to neighboring cells.

We propose a cell which is composed of coupled quantum dots occupied by two electrons [7]. The requisite bistability is accomplished through the interaction of quantum confinement effects, the Coulomb interaction between the two electrons, and the quantization of charge [8]. The intercellular interaction is provided by the Coulomb repulsion between electrons in different cells. We analyze this cell and the interactions between neighboring cells in Section 2.

In Section 3 we propose a new paradigm for how computation could be done with an array of quantum devices. Because no direct connections can be made to interior cells, information or *energy* can enter the array only from the edges. *Edge-driven computation* imposes further constraints on the nature of the computing process [9]. The lack of direct connections to the interior cells also means that no mechanism exists for keeping the array away from its equilibrium ground-state configuration. We are therefore led to use the ground-state of the array to do the computation. *Computing with the ground state* means that the physics of the array must perform the computation by dissipating energy as it relaxes to the ground state. This has the distinct advantages that the computing process is independent of the details of the energy relaxation mechanisms and that the unavoidable energy dissipation is useful to the computing process.

Section 4 demonstrates that QCA's can perform useful functions. We show how logical gates and inverters can be constructed with arrays of the two-electron bistable quantum cell we propose. Section 5 discusses some key issues in realizing QCA's as a viable technology and Section 6 identifies technological advantages that a successful QCA implementation would enjoy.

2. Few-electron Quantum Cells

The specific cell we consider here is shown in Figure 1. Four quantum dots are coupled to a central dot by tunnel barriers. The two electrons tend to occupy antipodal sites in one of two configurations, shown in the figure as the *P=+1* and *P=-1* configurations. Our analysis below will show that the cell is indeed in one of these two stable states, and that an electrostatic perturbation, perhaps caused by neighboring cells, switches the cell between these two states in a very abrupt and nonlinear way. This permits the encoding of bit information in the cell.

The essential ingredients that produce the bistable saturation behavior [10] so desirable are 1) quantum confinement, 2) Coulomb interaction between electrons, 3) few-electron quantum mechanics, and 4) the discreteness of electronic charge.

A model for the quantum cell

We model the cell shown in Figure 1 using a Hubbard-type Hamiltonian. For the isolated cell, the Hamiltonian can be written,

$$H_0^{cell} = \sum_{i,\sigma} E_{0,i} n_{i,\sigma} + \sum_{i,\sigma} t(a_{i,\sigma}^\dagger a_{0,\sigma} + a_{0,\sigma}^\dagger a_{i,\sigma}) +$$

$$\sum_i E_Q n_{i,\uparrow} n_{i,\downarrow} + \sum_{i>j,\sigma,\sigma'} V_Q \frac{n_{i,\sigma} n_{i,\sigma'}}{|\vec{R}_i - \vec{R}_j|} \qquad . \tag{1}$$

Here $a_{i,\sigma}$ is the annihilation operator which destroys a particle at site *i* (i=0,1,2,3,4) with spin σ. The number operator for site *i* and spin σ is represented by $n_{i,\sigma}$. The on-site energy

P = +1   P = -1

FIGURE 1. The quantum cell consisting of five quantum dots which are occupied by two electrons. The mutual Coulombic repulsion between the electrons results in bistability between the P=+1 and P=-1 states.

for the ith dot is $E_{0,i}$; the coupling to the central dot is t; the charging energy for a single dot is E_Q. The last term represents the Coulombic potential energy for two electrons located at sites i and j at positions R_i and R_j. Unless otherwise noted, we will consider the case where all the on-site energies are equal, $E_{0,i}=E_0$.

For our standard model cell, on which the numerical results reported here are based, we obtain the values of the parameters in the Hamiltonian from a simple, experimentally reasonable model. We take each site to be a circular quantum dot with diameter $D=10\ nm$, and take E_0 to be the ground state energy of such a dot holding an electron with effective mass $m^* = 0.067\ m_0$. The near-neighbor distance between dot centers, a, is taken to be $20\ nm$. The Coulomb coupling strength, V_Q, is calculated for a material with a dielectric constant of 10. We take $E_Q=V_Q/(D/3)$ and $t=0.3\ meV$.

It is useful to define a quantity which represents the degree to which the charge density for a given eigenstate of the system is aligned linearly. This alignment could be either along the line through sites 1 and 3 or along the line through sites 2 and 4. For each site, we calculate the single particle density ρ_i, which is simply the expectation value of the total number operator for the two-electron eigenstate. The polarization, P, is defined as

$$P = \frac{(\rho_1 + \rho_3) - (\rho_2 + \rho_4)}{\rho_0 + \rho_1 + \rho_2 + \rho_3 + \rho_4} \quad . \tag{2}$$

For an isolated cell with all on-site energies equal, no polarization is preferred. We will see below that perturbations due to charges in neighboring cells can result in a strongly polarized ground state. The polarization thus defined is not to be confused with the usual dipole polarization of a continuous medium. It simply represents the degree to which the electrons in the cell are aligned and in which of the two possible directions the alignment occurs. For the states of interest here, the cell has no dipole moment.

The interaction of the cell with the surrounding environment, including other neighboring cells, is contained in a second term in the Hamiltonian which we write as H_{inter}^{cell}. We solve

the time independent Schrödinger equation for the state of the cell, $|\Psi_n\rangle$, under the influence of the neighboring cells:

$$(H_0^{cell} + H_{inter}^{cell})|\Psi_n\rangle \; = \; E_n|\Psi_n\rangle \; . \tag{3}$$

The spins of the two electrons can be either aligned or anti-aligned, with corresponding changes in the spatial part of the wavefunction due to the Pauli principle. We will restrict our attention to the case of anti-aligned spins here because that is the ground-state configuration; the spin-aligned case exhibits nearly identical behavior. The Hamiltonian is diagonalized directly in the basis of few-electron states. We calculate single particle densities, ρ_i, from the two-particle ground-state wavefunction $|\Psi_0\rangle$,

$$\rho_i \; = \; \sum_\sigma \langle\Psi_0|n_{i,\,\sigma}|\Psi_0\rangle \, , \tag{4}$$

and from the densities calculate the resultant polarization P (EQ. 2). To maintain charge neutrality, a fixed positive charge, $\tilde{\rho}$, with magnitude *(2/5)e* is assumed at each site. For the isolated cell, this has no effect and is included in the on-site energies. For several cells in close proximity, as will be considered below, the maintenance of overall cell charge neutrality means that the intercellular interaction is due to dipole, quadrupole, and higher moments of the cell charge distribution. If cells had a net total charge then electrons in cells at the periphery of a group of cells would tend to respond mostly to the net charge of the other cells.

The cell-cell response function

To be of use in a CA architecture, the polarization of one cell must be strongly coupled to the polarization of neighboring cells. Consider the case of two nearby cells shown in the inset to Figure 2. Suppose we fix the charge distribution in the right cell, labeled cell *2*. We assume cell *2* has polarization P_2, and that the charge density on site *0* is negligible (this means the charge density is completely determined by the polarization). For a given polarization of cell *2*, we can compute the electrostatic potential at each site in cell *1*. This
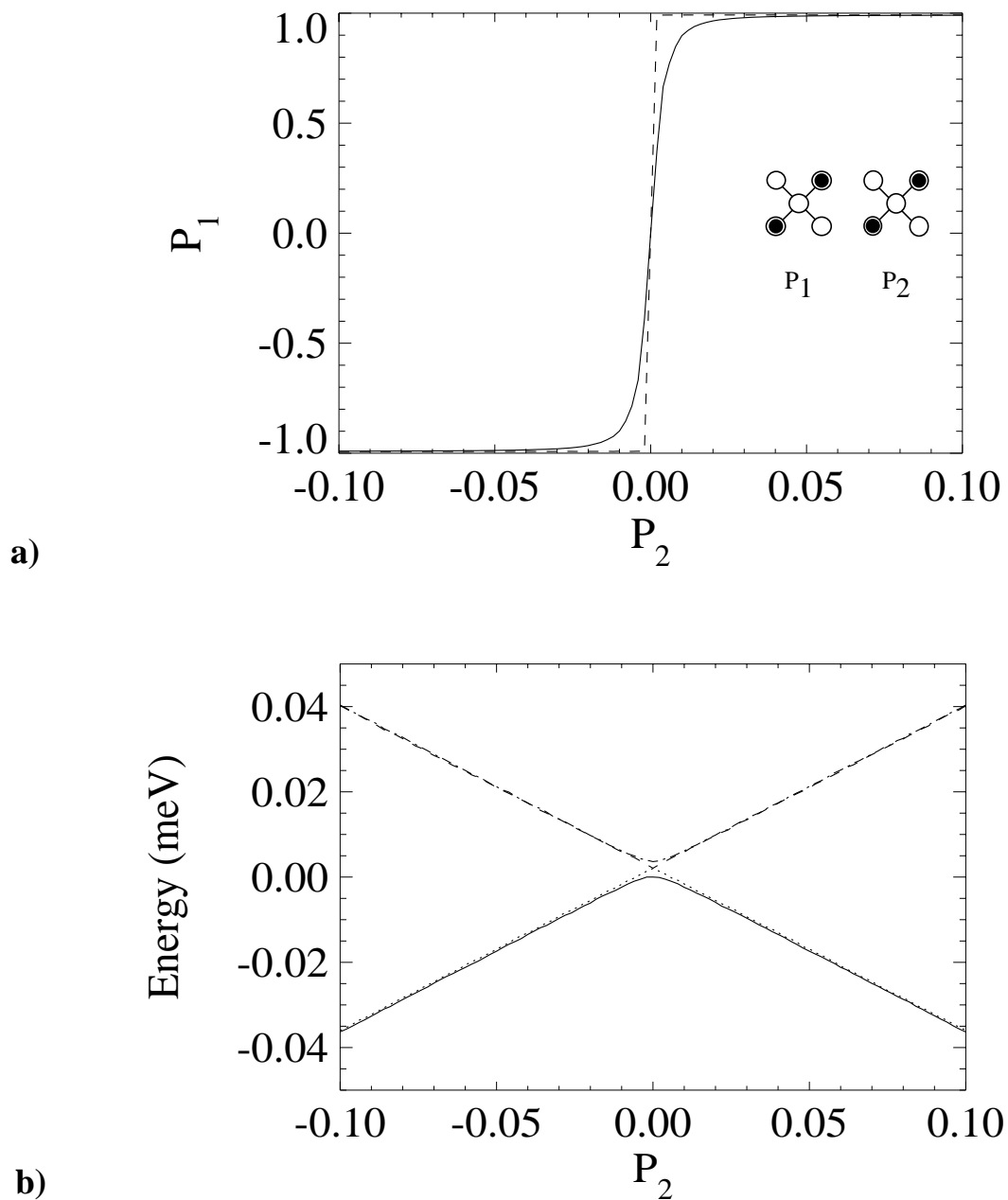
a)

b)

FIGURE 2. **The cell-cell response function. The polarization of the right cell is fixed and the induced polarization in the left cell is calculated. The top figure shows the calculated polarization of cell 1 as a function of the polarization of cell 2. Note that the range of P_2 shown is only from -0.1 to +0.1. This is because the transition in the induced polarization is so abrupt. The lower figure shows the first four eigen-energies of cell 1. The polarization of the lowest two are shown in the first figure.**

additional potential energy is then included in the total cell Hamiltonian. Thus the perturbing Hamiltonian is

$$H_{inter}^{cell} = H_1^{cell} = \sum_{i \in cell\ 1, \sigma} V_i^1 n_{i,\sigma},$$ (5)

where

$$V_i^m = \sum_{k \neq m, j} V_Q \frac{(\rho_j - \tilde{\rho})}{\left|\vec{R}_{k,j} - \vec{R}_{m,i}\right|}$$ (6)

is the potential at site i in cell m due to the charges in all other cells k. We denote the position of site j in cell k as $\vec{R}_{k,j}$. The total Hamiltonian for cell 1 is then

$$H^{cell} = H_0^{cell} + H_1^{cell}.$$ (7)

The two-electron Schrödinger equation is solved using this Hamiltonian for various values of P_2. The ground state polarization of cell 1, P_1, is then computed as described in the previous section.

Figure 2b shows the lowest four eigen-energies of cell 1 as a function of P_2. The perturbation rapidly separates states of opposite polarization.The excitation energy for a completely polarized cell to an excited state of opposite polarization is about *0.8* meV for our standard cell. This corresponds to a temperature of about 9 K. Figure 2a shows P_1 as a function of P_2 — the cell-cell response function. A very small polarization in cell *2* causes cell *1* to be very strongly polarized. This nonlinear response is the basis of the CA's we describe here. As the figure shows, the polarization *saturates* very quickly. This observation yields two important results:

1. ***The bipolar saturation means that we can encode bit information using the cell***
   polarization. A cell is almost always in a highly polarized state with $P \approx \pm 1$. We
   define the P=+1 state as a bit value of 1 and the P=-1 state as a bit value of 0. Only
   if the electrostatic environment due to other cells is nearly perfectly symmetric will
   there be no polarization.

2. ***The polarization of one cell induces a polarization in its neighbor.*** Figure 2
   shows that even a very slight polarization will induce nearly complete polarization
   of a neighboring cell. This cell-cell Coulomb coupling provides the mechanism for
   CA-like behavior. The rapid saturation of the cell-cell response function is
   analogous to the gain necessary to preserve digital logic levels from stage to stage.

The abruptness of the cell-cell response function depends on the ratio of the dot-to-dot
coupling energy, t in Eq. (1), to the Coulomb energy for electrons on different sites. The
magnitude of the coupling depends exponentially on both the distance between the dots
and the height of the potential barrier between them [11], each of which can be adjusted as
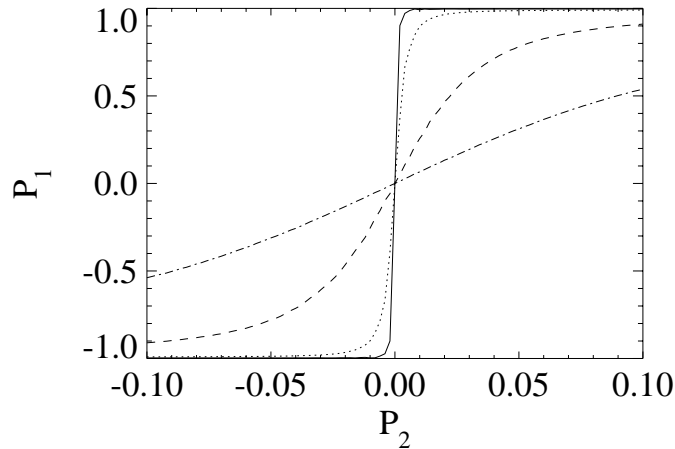engineering parameters. Figure 3 shows how the cell-cell response function varies with t.

FIGURE 3. The cell-cell response function for various values of the dot-to-dot coupling energy (t in Eq.1). The induced cell polarization P_1 is plotted as a function of the neighboring cell polarization P_2. The results are shown for values of the coupling energy, t=-0.2 (solid),-0.3 (dotted),-0.5 (dashed), and -0.7 (dot-dashed) meV. Note that the response is shown only for P_2 in the range [-0.1, +0.1].

Self-consistent analysis of several quantum cells

In the analysis of the previous two sections, the two-electron eigenstates were calculated for a single cell. It is important to note that for the Hamiltonian employed, these are exact two-particle eigenstates. Exchange and correlation effects have been included exactly. This was possible because we could explicitly enumerate all possible two-electron states and diagonalize the Hamiltonian in this basis set. We want to analyze clusters and arrays of cells to investigate possible device architectures. To do so we need to calculate the ground-state wavefunction of a group of cells. Exact diagonalization methods are then no longer tractable because the number of possible many-electron states increases so rapidly as the number of electrons increases. We must therefore turn to an approximate technique.

The potential at each site of a given cell depends on the charge density at each site of all other cells. We will treat the charge in all other cells as the generator of a Hartree-type potential and solve iteratively for the self-consistent solution in all cells. This approximation, which we call the Intercellular Hartree Approximation (ICHA), can be stated formally as follows. Let Ψ_0^k be the two-electron ground-state wavefunction for cell k, and ρ_j^m be the single particle density at site j in cell m. We begin with an initial guess for the densities. Then, for each cell we calculate the potential due to charges in all other cells.

$$V_i^k = \sum_{m \neq k, \, j} V_Q \frac{(\rho_j^m - \tilde{\rho})}{\left| \vec{R}_{m,\, j} - \vec{R}_{k,\, i} \right|}. \tag{8}$$

Although the neighboring cells will normally dominate this sum, we do not examine only near-neighbors but include the effect of all other cells. For each cell k, this results in a perturbation of the basic cell Hamiltonian of equation (1):

$$H_k^{cell} = \sum_{i \in cell \, k, \, \sigma} V_i^k n_{i,\, \sigma}. \tag{9}$$

The Schrödinger equation for each cell is now solved for the two-electron ground state eigenfunction:

$$(H_0^{cell} + H_k^{cell})|\Psi_0^k\rangle = E_0^k|\Psi_0^k\rangle .\tag{10}$$

From the ground state eigenfunctions we calculate the improved single particle densities.

$$\rho_j^k = \sum_\sigma \langle\Psi_0^k|n_{j,\sigma}|\Psi_0^k\rangle\tag{11}$$

The improved densities are then used in Equation (8) and the system is iterated until convergence is achieved. Once the system converges, the many-electron energy, E_{total}, is computed from the sum of the cell eigen-energies using the usual Hartree correction term to account for over-counting of the Coulomb interaction energy between cells:

$$E_{total} = \sum_k E_k^0 - \sum_{k>q,\,i,\,j} V_Q \frac{\rho_i^k \rho_j^q}{\left|\vec{R}_{k,\,i} - \vec{R}_{q,\,j}\right|} .\tag{12}$$

It should be stressed that the ICHA still treats Coulombic, exchange, and correlation effects between electrons in the *same* cell exactly. The Hartree mean field approach is used to treat self-consistently the interaction between electrons in *different* cells. Since electrons in different cells are physically distinguishable (there being no wavefunction overlap), the exchange coupling between them is zero. The Hartree and Hartree-Fock approximations are therefore equivalent in this case.

The converged ICHA solution will be an (approximate) eigenstate of the entire system. In general, however, it need not be the ground state. As with the usual Hartree approximation, which of the eigenstates the scheme converges to is determined by the choice of the initial guess. To find the ground state we must try many initial state guesses and determine which converged solution has the lowest energy. Typically, this does not present a serious problem for the type of cellular arrays considered here because the set of likely ground states is easily discerned. In general, a systematic search may be required.

The procedure described above uses, at each stage of the iteration, only the ground-state wavefunction of each cell. If all the excited states of the entire system were desired, we would have to include states composed of excited cell states as well. Since our interest is

in the ground-state, this is not necessary. It is relevant to point out however, that because each cell is in a "local" ground state, we do not require coherence of the many-electron wavefunction across the whole array of cells. All that is required to support this analysis is that the wavefunction is *coherent across a single cell*. No information about the phase of the wavefunction in other cells is relevant to the wavefunction in a given cell — only the charge densities in other cells need be known.

3. Computing with Quantum Cellular Automata

We present a new paradigm for computing with quantum cellular automata. This represents a complete picture of how quantum devices could be coupled in a CA architecture to perform useful functions. The paradigm we propose is shown schematically in Figure 4. We will focus on the zero temperature case; temperature effects will be considered below. As shown in the figure, the inputs are along an edge of the array. Specifying the inputs consists of electrostatically fixing the polarization of the input cells. This could be accomplished by simply applying voltages to conducting "set" lines which come in close proximity to the cells, but any method that fixes the cell polarization state would do. The output cells are not fixed; their polarization state is sensed, perhaps by electrostatic coupling to "sense" lines. There could also be several input and output edges. Computation proceeds in the following steps:
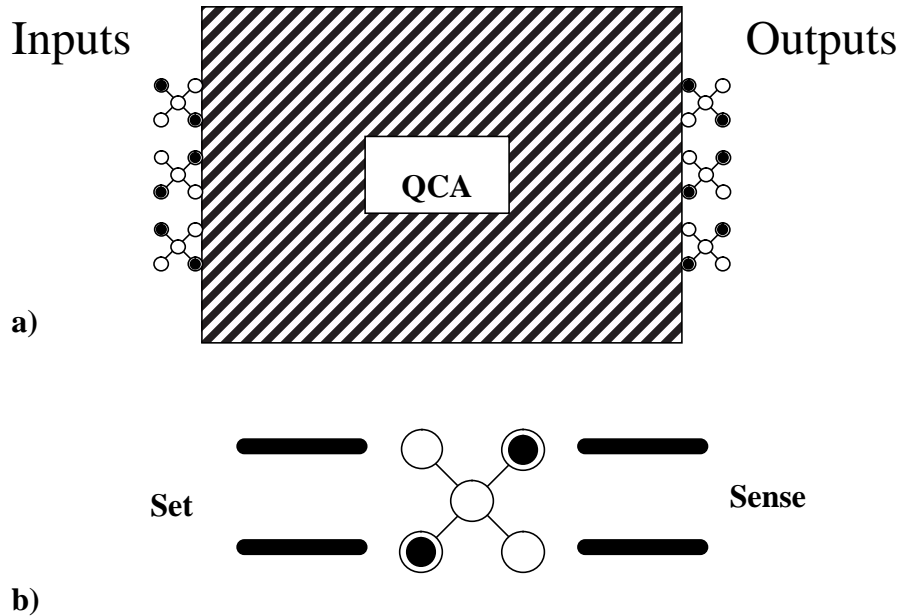

FIGURE 4. The new paradigm for computing with quantum cellular automata. The input to the QCA is provided at an edge by setting the polarization state of the edge cells (*edge-driven computation*). The QCA is allowed to dissipatively move to its new ground-state configuration and the output is sensed at the other edge (*computing with the ground state*). The "set" and "sense" lines are shown schematically.

1. Write the input bits by fixing the polarization state of cells along the input edge (edge-driven computation).

2. Allow the array to relax to its ground state with these inputs (computing with the ground state).

3. Read the results of the computation by sensing the polarization state of cells at the output edge.

The essential elements that define this computing paradigm are *computing with the ground state* and *edge-driven computation*, which we discuss below.

Computing with the Ground State

The advantage of computing with the ground state is that it leaves the computing process insensitive to the details of the dissipative processes which couple the electrons in the array to the environment. Consider a QCA at zero temperature for which all the input cells have been held in a fixed state. Dissipative processes have brought the array to its ground state configuration for these boundary conditions. Suppose at time $t=0$ the input cell states are set to their new input values completely abruptly. Just after the inputs are applied at the edge of the QCA, the array is no longer in the ground state but is now in an excited non-stationary state for the new boundary conditions. In the time between 0 and t_r, a characteristic relaxation time, various dissipative processes will bring the array to its new ground-state configuration. After that, the array will be stable until the boundary conditions are changed again. During the relaxation time the temporal evolution of the system is *very* complicated. Even without dissipation, the system will undergo quantum oscillations due to interference between the various eigenstates which compose the $t=0^+$ state. The dissipative processes, like phonon emission, introduce extraordinary complication in the temporal evolution. The exact state of the system at a particular time $t<t_r$ depends not just on phonon emission rates, but on the *particular* phonons emitted by

these *particular* electrons. In short, the temporal evolution before $t=t_r$ depends on the precise microscopic details of the dissipative dynamics. By contrast, *the ground state configuration to which the system relaxes is completely independent of the dissipation mechanisms*. Hence we choose to do computing with the ground state only.

Edge-driven Computation

In the QCA computing paradigm we are proposing, the input data is represented by edge cells whose polarization is fixed. Computing then proceeds by allowing the physics interior to the QCA to "solve" the dissipative many-electron problem for this new set of boundary conditions. The array is designed so the part of the ground-state "solution" of the many-body problem which appears at the output edge corresponds to the solution of the computing problem posed by the input data.

The advantage of writing input and reading output only at the edges of the array is that no separate connections to the array interior need be made. Because quantum devices are of necessity extremely small, the problem of making contacts to each element or device becomes severe. If a single array contains thousands of individual cells, the "wiring" problem is overwhelming.

Edge-driven computation is, in fact, the practical requirement which makes *computing with the ground state* necessary. If no connections can be made to the interior of the array, there is no controlled mechanism for keeping the system away from the ground state. Neither clocking nor refresh mechanisms are available. With a change in input, the system will dissipate energy and find a new equilibrium ground state. The only choice is whether to try to do computation with the system's transient response, or with its ground state. For the reasons discussed above, the ground-state approach is preferable.

Conventional computing, by contrast, is done using very highly-excited, non-equilibrium states. Because each element (device) can be separately contacted, energy can be fed into

the system at each point. The entire system can thereby be maintained in non-equilibrium states. The advantage of this is that the energy difference between the states used for computing can be very much larger than $k_B T$. The requirement that each element be driven far from equilibrium ultimately contributes to the difficulty of reducing the scale of conventional technology to the nanometer level. The breakdown of the operating device physics at small scales also plays a crucial role in the scale-down problem.

Ultimately, temperature effects are the principal problem to be overcome in physically realizing the QCA computing paradigm. The critical energy is the energy difference between the ground state and the first excited state of the array. If this is sufficiently large compared with $k_B T$, the system will be reliably in the ground state after time t_r. Fortunately, this energy difference increases quadratically as the cell dimensions shrink. If the cell size could be made a few Angstroms, the energy differences would be comparable to atomic energy levels — several electron volts! This is, of course, not feasible with semiconductor implementations, but may ultimately be attainable in molecular electronics. It may, however, be possible to fabricate cells in semiconductors small enough to work reliably at reasonable cryogenic temperatures.

Relation to synchronous CA rules

The relationship between the Quantum Cellular Automata described here and traditional rule-base CA's is not direct. Cellular automata are usually described by a set of CA rules which govern the temporal evolution of the array [12]. Time proceeds in discrete increments called generations. The rules determine the state of the array based on its configuration in the previous generation. Clearly, for the QCA described here, the temporal evolution proceeds not through discrete generations but through continuous physical time. Moreover, as argued above, we are not particularly interested in the temporal evolution of the QCA in order to do computing. We are only concerned with the final ground state configuration associated with a particular input state. Like the rule-based

synchronous CA, the QCA is an array of interacting multi-state cells and the behavior is dominated by near-neighbor interactions between cells. Thus, the QCA is chiefly related to traditional CA's by *analogy.*

Nevertheless, it is possible to construct a rule-based CA from the QCA interacting cell Hamiltonian (Eq. 10). The CA so constructed may be useful, perhaps not in describing the transient state of the QCA, but rather in calculating the ground state configuration, which is our primary concern anyway.

CA rules from the Schrödinger equation

The CA rule set is constructed as follows. For each cell, consider all possible polarization states ($P = \pm 1$) of the neighbors (neighbors out to any distance useful can be considered). For each configuration of the neighboring polarization, solve the Schrödinger equation (Eq. 10) and determine the target cell ground-state and its polarization. The map of neighbor polarizations to target cell polarization constitutes the CA rule set for that particular target cell. In general, a different rule set may apply to each cell. Typically, many cells will have similar environments and use the same rules.

The rule set obtained by this procedure can be recast in terms of a *weighted voting* procedure. In deciding the state of a particular cell, the neighboring cells vote according to their own state. The votes are weighted differently depending on the geometrical relationship between each neighbor and the target cell. The votes of closer cells are weighted more heavily than those of more distant cells. In addition, the weights can be negative, indicating that the energetics of the interaction between the neighbor and the target cell favor them having opposite polarizations. The CA rules generated by the solution of the Schrödinger equation for the target cell can then recast in the form of voting weights for the neighbors. Any set of voting weights which reproduces the CA rule set is equivalent.

Extended CA rules

This procedure so far has one problem which can be remedied by expanding the rules slightly. It is possible for the votes of the neighbors to result in a "tie". That is, the neighboring polarizations may be arranged so symmetrically that the ground-state polarization of the target cell is zero. It is desirable to break this tie by consulting the immediate history of the neighbors. The neighbors which flipped their polarization in the preceding generation are simply weighted more heavily than those which have not flipped. This introduces a notion of momentum which is otherwise absent in a two-state CA. With these *momentum rules*, ties are still possible but are now exceedingly rare events that can be handled by tie-breaking with a random number.

The CA rules corresponding to a particular QCA are thus derived from the Schrödinger equation and augmented by the momentum rule discussed above. The evolution of the synchronous CA is still not directly related to the temporal evolution of the physical QCA. The CA rules know nothing of the details of the dissipative dynamics, for example. However, in our experience, the synchronous CA with the momentum rules can be useful in determining the ground state of the QCA. If we start with a stable QCA state, and then flip the input cells to correspond to the new input condition, the synchronous CA will evolve to a stationary state which corresponds to the ground state of the physical QCA. That the final state is really the ground state can be checked by using the more rigorous self-consistent calculations described in the previous section.

4. Device Applications

Two types of QCA structures for computing can be envisioned. One type is a very large regular array of cells. We have work in progress exploring this type of array. It is widely appreciated that doing computing with large regular CA's is a significant challenge, particularly with a simple rule set. The solution to this difficult problem may have the greatest long-term potential, however, for exploiting the massive parallelism inherent in the QCA paradigm.

A second type of QCA structure involves a highly irregular array of cells. We show below that using simple irregular arrays one can produce structures analogous to wires, inverters, AND gates and OR gates. Since these can be connected together, more-complex devices such as adders and multipliers can be constructed. Because the individual devices are so small, this represents a potentially enormous increase in functional density in an architecture free of the usual interconnect problems. We examine below how these basic logical gates can be constructed from quantum cells.

The device configurations shown are the results of self-consistent calculations of the ground state using the ICHA described above. The figures show the calculated ground-state charge density on each site of the cellular array. In these figures the dot diameters reflect the relative electron density at each site (dot) in the cell.
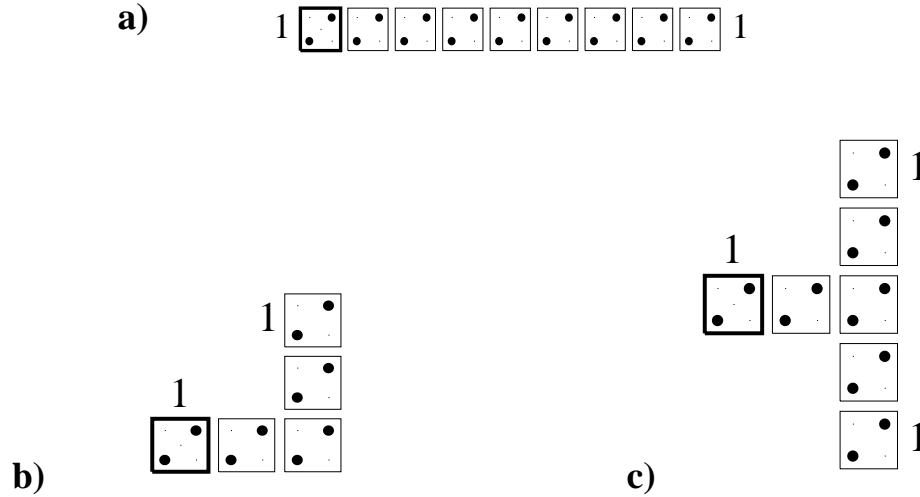
a)

b)

c)

FIGURE 5. QCA wires. a) The basic wire. b) A corner in a wire. c) Fan-out of one signal into two channels. In each case the darker (left-most) cell has a fixed polarization which constitutes the input. Note that these figures are not simply schematic, but are a plot of the results of a self-consistent many-body calculation of the ground state for the cellular array. The diameter of each circle is proportional to the calculated charge density at each site.

Wires

A linear chain of cells oriented as shown in Figure 5a functions as a wire, transmitting a 0 or 1 (P=+1 or P=-1) from one end of the wire to the other. This is demonstrated by fixing the polarization of one end (the left), while letting the other end be unconstrained, and calculating the self-consistent ground state of the chain using the ICHA method. Figure 5a shows the results of that calculation. Not surprisingly, the ground state consists of all cells aligned with the same polarization as the end cell. The first excited state of the chain has a "kink" in it at the chain center, *i.e.*, half the cells polarized one way and half polarized the other. For our example, the energy of the first excited state is about *1* meV ($\Delta E/k_B T = 10\ K$) above the ground state energy. Wire bends and fan-out are also possible, as shown in Figures 5b and 5c respectively. Again, the left-most cell is fixed and the ground-state configuration calculated. This sort of fan-out is appropriate for the edge-driven paradigm discussed above.
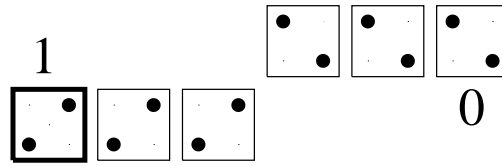
FIGURE 6. An inverter constructed from a quantum cell automaton.

Inverter

By offsetting one chain of cells from another, as shown in Figure 6, an inverter can be constructed. If the polarization of the one end is fixed, the polarization of the other end will be opposite.

AND and OR gates

AND and OR gates can be made from the intersection of two wires. Figure 7 shows an OR gate. The darker boxes are around the input cells. Their polarization is set to correspond to
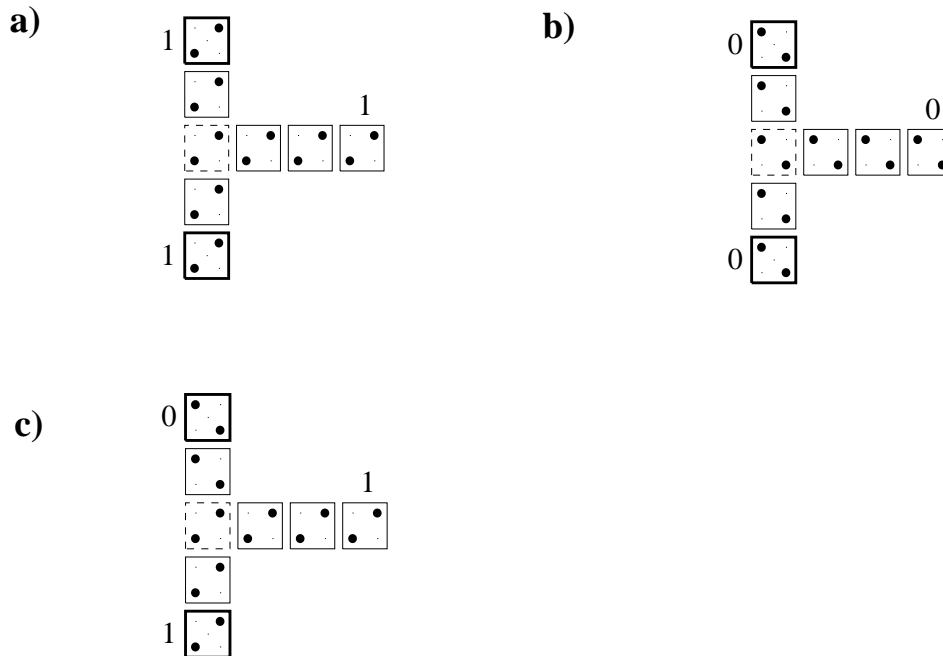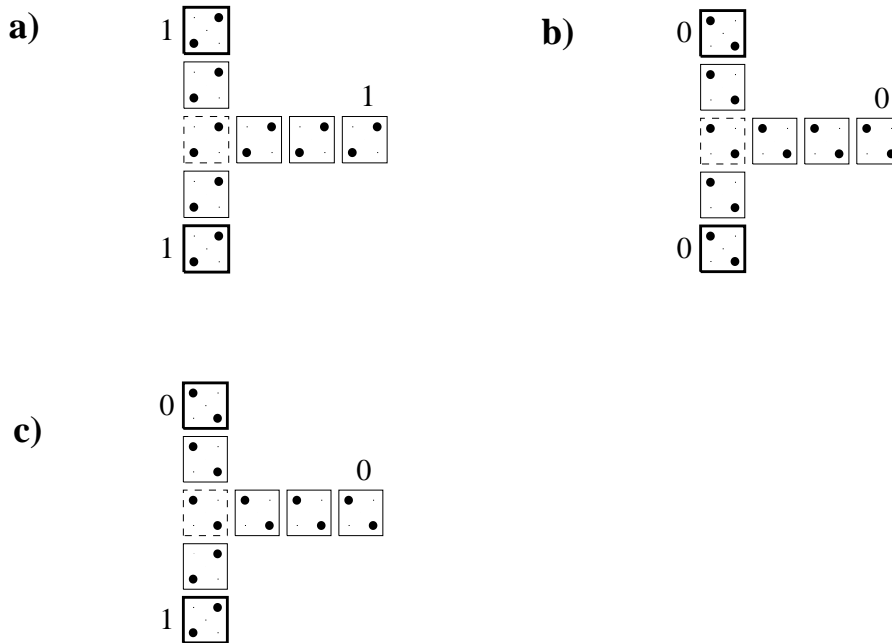

FIGURE 7. An OR gate. The cells in darker squares are fixed to the input states. The cell in the dashed square is biased slightly toward the "1" state.

the logical values shown. For the case when the inputs are *0* and *1* (Figure 7c), the central cell state would normally be indeterminate since a "tie vote" exists between the input cells. To resolve, this we *bias* the central cell by increasing the site energy on sites *2* and *4* slightly. This could be accomplished by making the quantum-dot diameter slightly smaller on these two sites. It is then slightly more energetically favorable for the cell to be in a *1* state, thus breaking the tie. The AND gate is constructed in exactly the same way except that the central cell is biased toward the 0 state. The AND gate is shown in Figure 8. Both these figures reflect the results of self-consistent solutions of the many-electron problem for the entire array shown.

FIGURE 8. An AND gate. The cells in darker squares are fixed to the input states. The cell in the dashed square is biased slightly toward the "0" state.

Memory cell

A single quantum cell can act as a memory storage cell. Once prepared in an eigenstate with $P=+1$, for example, the cell will in principle remain in that configuration indefinitely. One problem is that slight variations in the potential environment may make it slip into the other eigenstates. To avoid this it may be desirable to use small or medium-size arrays of quantum cells to store each bit. This is shown schematically in Figure 9. One advantage of a regular rectangular array of cells is that it may be possible to use the interaction of many cells with the set and sense lines (the exact mechanism for setting and sensing is not critical here). The problem of making non-interfering address lines is certainly non-trivial.
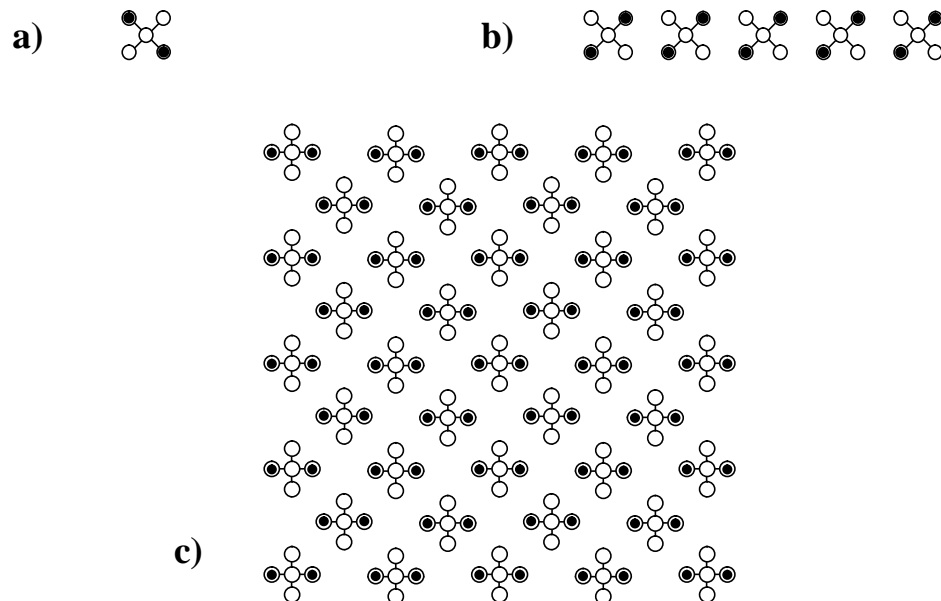
FIGURE 9. Quantum cellular arrays as memory storage cells. A single bit can be stored in a) a single cell, b) a line of cells, or c) an array of cells. Arrays of cells would make the storage more robust.

5. Issues for QCA as a Technology

Fabrication of QCA's in semiconductors appears to be within reach of current technology. The GaAs/AlGaAs system has proven fruitful as a means of fabricating quantum dot structures by imposing electrostatically a pattern on the two-dimensional electron gas formed at the heterojunction interface. Other materials systems, including molecular systems, are also candidates for realizing a QCA structure. Any implementation must deal with several issues key to the successful operation of the cell we have described.

Uniformity of cell occupancy

It is important for the operation of the QCA that each cell contain two electrons. The cell-cell response function degrades significantly if one or three electrons are in a cell. Fortunately, the physics of the cell acts to ensure that the occupancy will be very uniform. This is so because the Coulomb interaction causes significant energy-level splitting between the different cell charge states. The Coulomb energy cost to add the third electron is on the order of 10 meV for cells with a *30 nm* separation. Experiments by Obermeyer *et al.* [13] have shown that uniformity in the number of electrons/dot can be maintained in arrays of 10^8 dots.

Dot-size control

The size of the fabricated quantum dots must be fairly well controlled. Variations in the size of the dots translates into variations in the confinement energies on each dot. The cell bistability occurs because the Coulomb interaction is determinative in selecting a preferred polarization state. If the magnitude of the variation among the dots in the confinement energies is greater than the Coulomb energies involved, the cell will be pinned at a fixed polarization. Note that dot size variations are critical only within a single cell; variations between different cells are easily tolerated.

Temperature

The temperature of operation is a major factor. Our QCA quantum cell is expected to work at liquid helium temperatures for dot dimensions which are within the capability of current semiconductor fabrication technology. As technology advances to smaller and smaller dimensions on the few-nanometer scale, the temperature of operation will be allowed to increase. Perhaps our envisioned quantum cellular automaton will find its first room temperature implementation in molecular electronics.

6. Technological Benefits

If successful, quantum cellular automata would represent a revolutionary, rather than evolutionary, departure from conventional electronics. In this section we review some possible benefits a QCA technology might provide.

Quantum cellular automata solve the interconnection problem. It is widely acknowledged that the main challenge to further improvements in microelectronics is the interconnection and wiring problem. The QCA we discuss accommodate this challenge in a natural fashion. Interconnect lines are no longer necessary to provide the communication between cells; the Coulomb interaction provides the coupling mechanism. *Edge-driven computation* requires neither energy nor information to be transmitted directly to interior cells. *Computing with the ground state* makes both clocking and refresh signals unnecessary.

Quantum cellular automata make possible ultra-high density computing elements. The chief technological advantage of the proposed structures is the improved functional density of computing elements. With a *10* nm design rule, the cell dimensions would be about *50* nm *x 50* nm, which translates into an extremely high packing density of about 10^{10} cells/cm^2. Since, as shown above, a single cell can function as a logical gate, this represents an extremely high functional density.

Quantum cellular automata are extremely low in power dissipation. High packing density is usually accompanied by high power dissipation. However, in QCA structures, the information is stored in physical systems close to their ground state. The energy input to the array is the energy required to set each input bit — about *1* meV per *input* bit. This energy is dissipated in the time it takes for the QCA to relax to its new ground-state configuration, probably less than a few picoseconds (phonon scattering times). This represents a power dissipation of roughly 10^{-10} Watts per input bit, much less than conventional devices.

Quantum cellular automata offer the possibility of ultra-fast computing. As estimated above, the computation occurs in a QCA over the relaxation time for the electrons in the array, probably on the order of picoseconds. It is clear that this relaxation time is a function of the electron-phonon coupling and represents a fundamental speed limit for doing computation with electrons in a semiconductor.

Quantum cellular automata may facilitate fabrication of ultra-dense memory storage. The QCA cell encodes a bit of information. Writing and reading the bit involves very low power dissipation and is very fast. While problems of cell addressing, and cell volatility appear challenging, the possibility of solid-state electronic storage of information at these densities invites further investigation.

Summary

We have presented a specific model for using nanoelectronic devices in a cellular automata architecture and proposed a new paradigm for computing in this framework. Each cell consists of a central quantum dot and four neighboring dots occupied by two electrons. The Coulomb repulsion between the two electrons, quantum confinement effects, and the discreteness of the electronic charge, combine to produce strongly polarized (in the sense defined above) ground states. The response of this polarization to the electrostatic environment is highly nonlinear and exhibits the bistable saturation necessary for a two-state CA. The concept of *edge-driven computation* solves the interconnection problem. The concept of *computing with the ground state* in the QCA approach permits ultra-fast operation, eliminates problems of interconnect delays, resistive and capacitive effects, power dissipation, and limited densities associated with conventional architectures.

ACKNOWLEDGEMENTS

REFERENCES

1. D. K. Ferry, L. A. Akers, and E. W. Greeneich, *Ultra Large Scale Interconnected Microelectronics* (Prentice Hall, Englewood Cliffs N.J., 1988).

2. For a recent overview see *Nanostructures and Mesoscopic Systems*, Wiley P. Kirk and Mark A. Reed (eds.), (Academic Press, Boston, 1992).

3. R. T. Bate, *Bull. Am. Phys. Soc*. **22**, 407 (1977).

4. J.N. Randall, M.A. Reed, and G.A. Frazier, *J. Vac. Sci. Technol*. **B7**, 1398, (1989).

5. *Granular Nanoelectronics*, David K. Ferry, John R. Barker, and Carlo Jacoboni (eds.), (Plendum, New York, 1991).

6. R. Landauer, *Phys. Today* **42**, 119 (1989).

7. A proposal for cells with single electron occupancy has been made, but lacks the requisite bistable character. See P. Bakshi, D.A. Broido, and K. Kempa, *J. Appl. Phys.* **70**, 5150 (1991).

8. Craig S. Lent, *Nanostructures and Mesoscopic Systems*, Wiley P. Kirk and Mark A. Reed (eds.), 183 (Academic Press, Boston, 1992).

9. The edge-driven paradigm proposed here is to be distinguished from conventional systolic architectures. In systolic arrays *information* is input only at the edges, but *energy* must be separately fed to each computational element, typically through power lines to

each cell. In the paradigm discussed here, both energy and information are supplied only to the edge cells.

10. K. Obermayer, G. Mahler, and H. Haken, *Phys. Rev. Lett.* **58**, 1792 (1987).

11. A one dimensional treatment is given at length in M. Morrison, T. Estle, and N. Lane, *Quantum States of Atoms, Molecules, and Solids*, chapter 13 (Prentice-Hall, New Jersey, 1976).

12. T. Toffoli and N. Margolus, *Cellular Automata Machines*: A New Environment for Modeling (MIT Press, Cambridge, Massachusetts, 1987).

13. B. Meurer, D. Heitmann, and K. Ploog, *Phys. Rev. Lett.* **68**, 1371 (1992).

Figure Captions

FIGURE 1. The quantum cell consisting of five quantum dots which are occupied by two electrons. The mutual Coulombic repulsion between the electrons results in bistability between the P=+1 and P=-1 states.
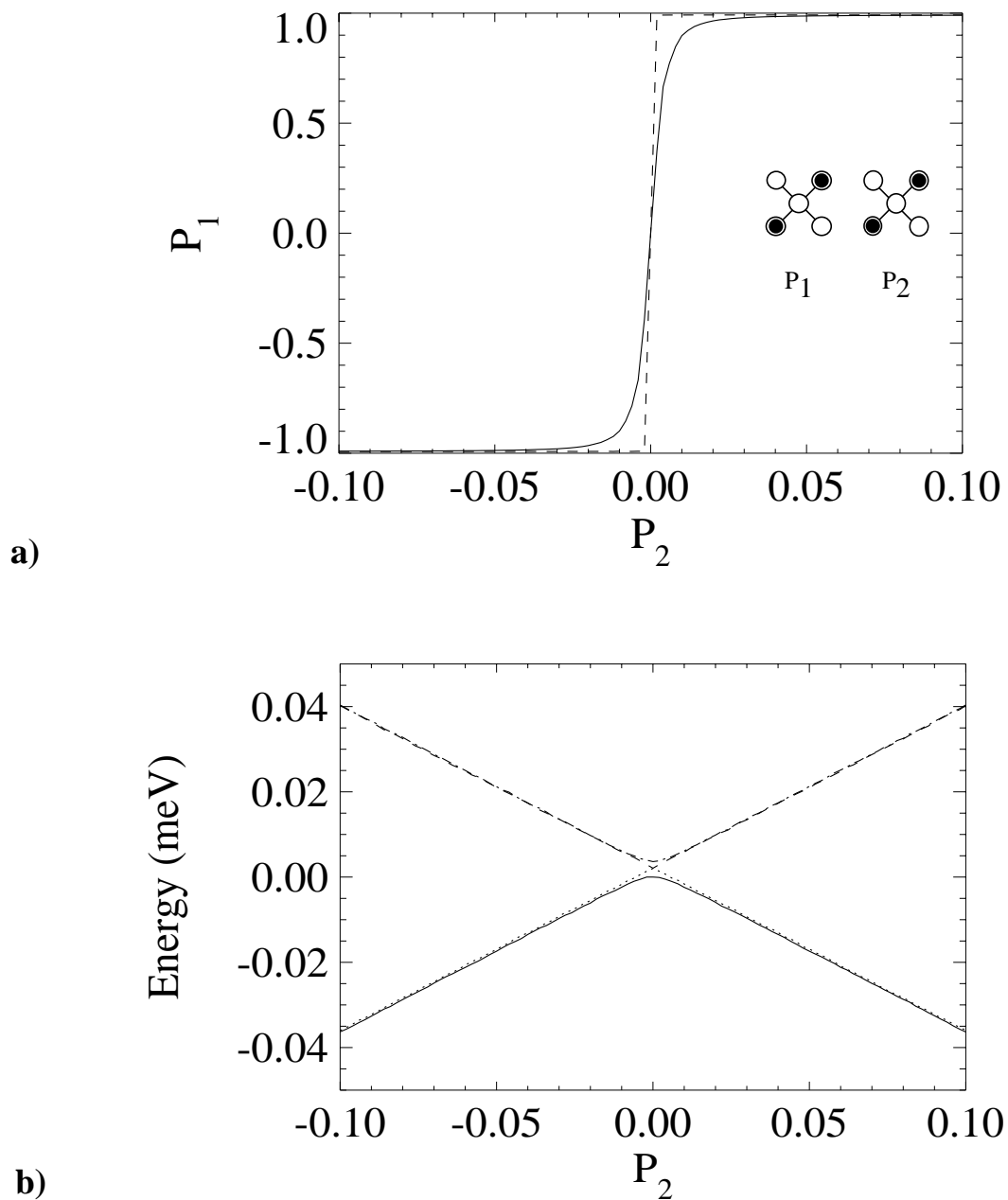
FIGURE 2. The cell-cell response function. The polarization of the right cell is fixed and the induced polarization in the left cell is calculated. The top figure shows the calculated polarization of cell 1 as a function of the polarization of cell 2. Note that the range of P_2 shown is only from -0.1 to +0.1. This is because the transition in the induced polarization is so abrupt. The lower figure shows the first four eigen-energies of cell 1. The polarization of the lowest two are shown in the first figure.

FIGURE 3. The cell-cell response function for various values of the dot-to-dot coupling energy (*t* in Eq.1). The induced cell polarization P_1 is plotted as a function of the neighboring cell polarization P_2. The results are shown for values of the coupling energy, *t*=-0.2 (solid),-0.3 (dotted),-0.5 (dashed), and -0.7 (dot-dashed) meV. Note that the response is shown only for P_2 in the range [-0.1, +0.1].

FIGURE 4. The new paradigm for computing with quantum cellular automata. The input to the QCA is provided at an edge by setting the polarization state of the edge cells (*edge-driven computation*). The QCA is allowed to dissipatively move to its new ground-state configuration and the output is sensed at the other edge (*computing with the ground state*). The "set" and "sense" lines are shown schematically.

FIGURE 5. QCA wires. a) The basic wire. b) A corner in a wire. c) Fan-out of one signal into two channels. In each case the darker (left-most) cell has a fixed polarization which constitutes the input. Note that these figures are not simply schematic, but are a plot of the results of a self-consistent many-body calculation of the ground state for the

cellular array. The diameter of each circle is proportional to the calculated charge density at each site.

FIGURE 6. An inverter constructed from a quantum cell automaton.

FIGURE 7. An OR gate. The cells in darker squares are fixed to the input states. The cell in the dashed square is biased slightly toward the "1" state.

FIGURE 8. An AND gate. The cells in darker squares are fixed to the input states. The cell in the dashed square is biased slightly toward the "0" state.

FIGURE 9. Quantum cellular arrays as memory storage cells. A single bit can be stored in a) a single cell, b) a line of cells, or c) an array of cells. Arrays of cells would make the storage more robust.

FIGURE 1. The quantum cell consisting of five quantum dots which are occupied by two electrons. The mutual Coulombic repulsion between the electrons results in bistability between the P=+1 and P=-1 states.

a)

b)

FIGURE 2. The cell-cell response function. The polarization of the right cell is fixed and the induced polarization in the left cell is calculated. The top figure shows the calculated polarization of cell 1 as a function of the polarization of cell 2. Note that the range of P_2 shown is only from -0.1 to +0.1. This is because the transition in the induced polarization is so abrupt. The lower figure shows the first four eigen-energies of cell 1. The polarization of the lowest two are shown in the first figure.

FIGURE 3. The cell-cell response function for various values of the dot-to-dot coupling energy (t in Eq.1). The induced cell polarization P_1 is plotted as a function of the neighboring cell polarization P_2. The results are shown for values of the coupling energy, t=-0.2 (solid),-0.3 (dotted),-0.5 (dashed), and -0.7 (dot-dashed) meV. Note that the response is shown only for P_2 in the range [-0.1, +0.1].
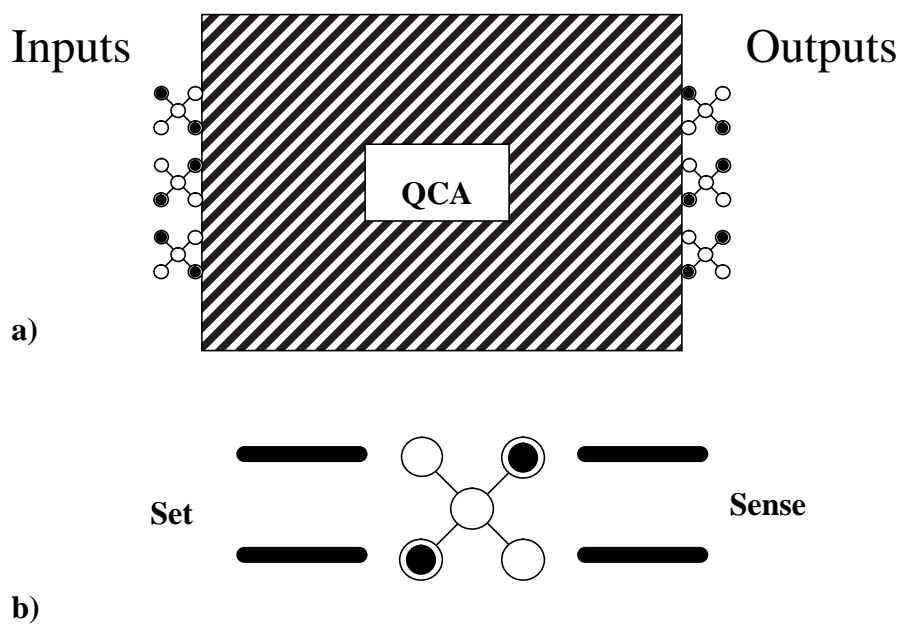
Inputs

Outputs

QCA

a)

Set

Sense

b)

FIGURE 4. The new paradigm for computing with quantum cellular automata. The input to the QCA is provided at an edge by setting the polarization state of the edge cells (*edge-driven computation*). The QCA is allowed to dissipatively move to its new ground-state configuration and the output is sensed at the other edge (*computing with the ground state*). The "set" and "sense" lines are shown schematically.
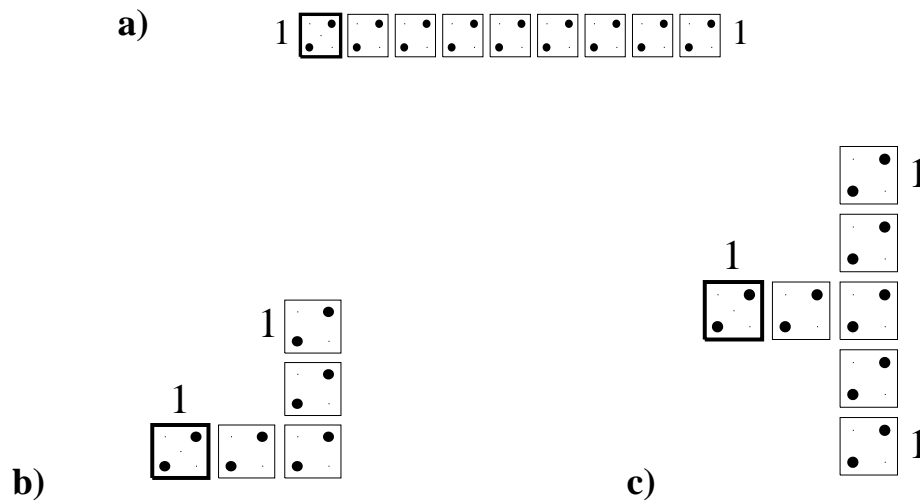
FIGURE 5. QCA wires. a) The basic wire. b) A corner in a wire. c) Fan-out of one signal into two channels. In each case the darker (left-most) cell has a fixed polarization which constitutes the input. Note that these figures are not simply schematic, but are a plot of the results of a self-consistent many-body calculation of the ground state for the cellular array. The diameter of each circle is proportional to the calculated charge density at each site.
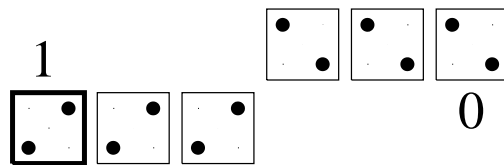
FIGURE 6. An inverter constructed from a quantum cell automaton.
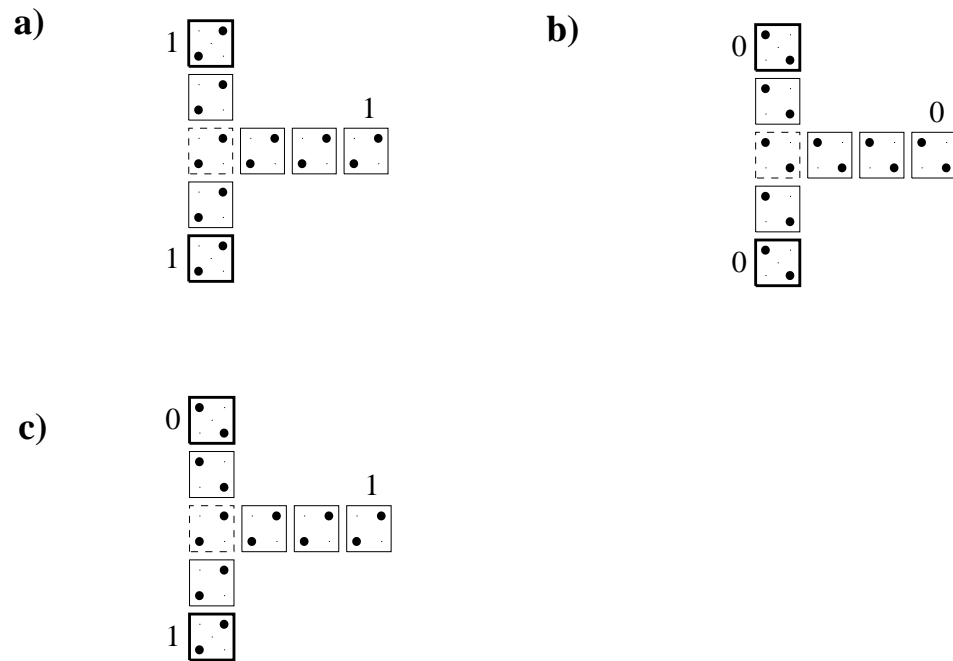
FIGURE 7. An OR gate. The cells in darker squares are fixed to the input states. The cell in the dashed square is biased slightly toward the "1" state.
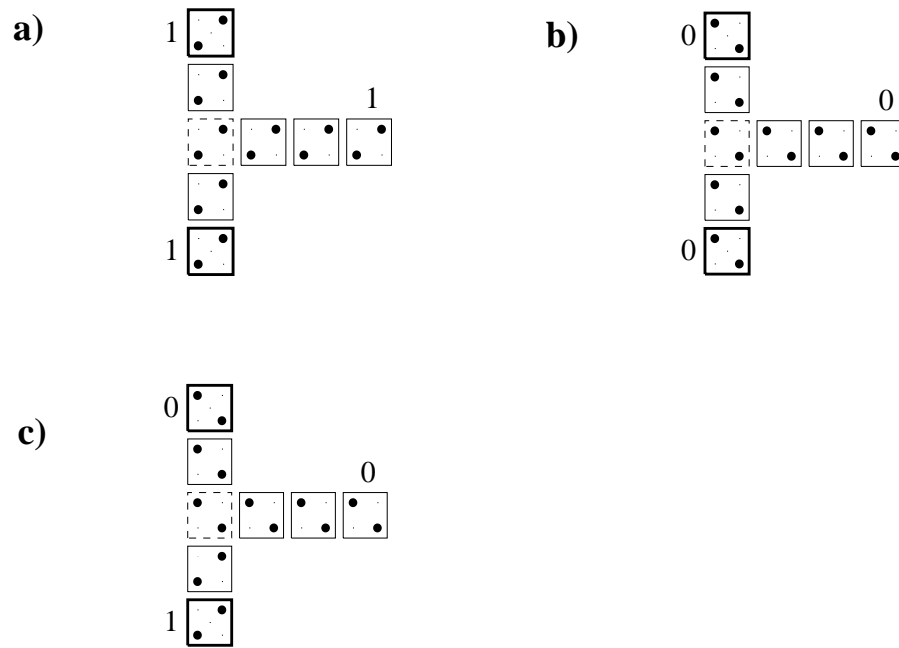
FIGURE 8. An AND gate. The cells in darker squares are fixed to the input states. The cell in the dashed square is biased slightly toward the "0" state.
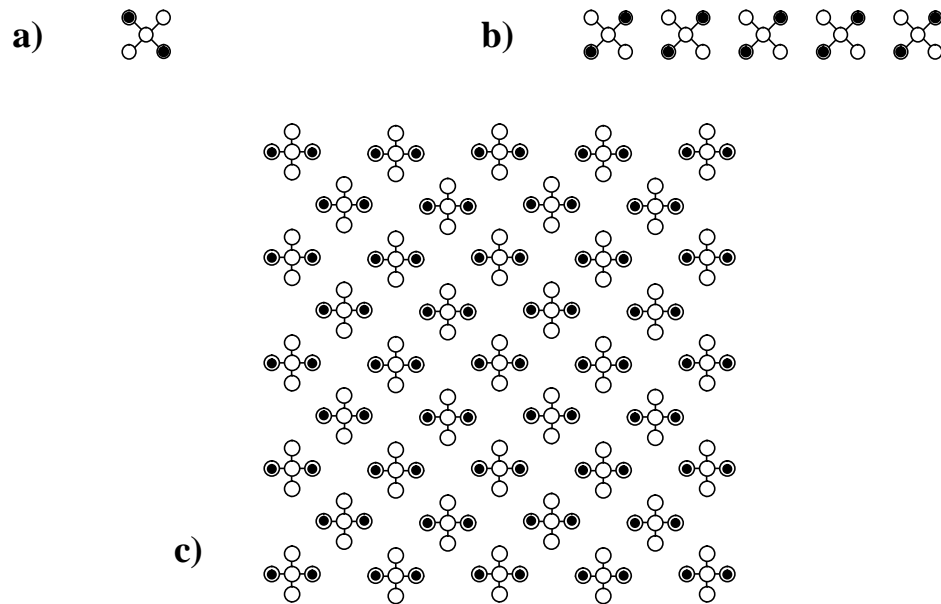
FIGURE 9. Quantum cellular arrays as memory storage cells. A single bit can be stored in a) a single cell, b) a line of cells, or c) an array of cells. Arrays of cells would make the storage more robust.